

# Comparison of recent rubber-elasticity theories with biaxial stress–strain data: the slip-link theory of Edwards and Vilgis

Bohumil Meissner\*, Libor Matějka

*Institute of Macromolecular Chemistry, Academy of Sciences of the Czech Republic, Heyrovsky Square 2, 16206 Prague 6, Czech Republic*

Received 18 May 2001; accepted 15 February 2002

## Abstract

The Edwards–Vilgis (EV) slip-link theory (1986) derives the elastic free energy of a rubber-like network model containing stable and sliding network junctions (crosslinks and slip-links) and predicts both low-strain softening and high-strain hardening. The four-parameter stress–strain relations calculated by the theory for geometrically different deformation modes up to high strains were tested experimentally using published biaxial stress–strain data on simple covalently crosslinked networks. For networks with low degrees of strain softening and low extensibilities, the experimental dependencies could be described rather well but, generally, a simultaneous satisfactory fit to uniaxial, pure shear and equibiaxial data was not obtained. Systematic experiment–theory deviations exceeding 10% were observed and some of the parameters had a tendency to assume values lying outside the reasonably expected range. The prediction of a pronounced maximum in the strain dependence of stress supported by slip-links seems to be a reason for the discrepancy. Also, modeling of the high-strain singularity in entropy is done in the EV theory using a rather simple approximation. As a result, the finite extensibility contribution to the stress of a slip-link-free network model becomes improbably high and significantly exceeds that following, at a given modulus and locking stretch, from the rigorously derived Langevin-statistics-based eight-chain-network elasticity theory of Arruda and Boyce. © 2002 Elsevier Science Ltd. All rights reserved.

*Keywords:* Theory of rubber elasticity; Biaxial deformations; Experimental testing

## 1. Introduction

The problem of obtaining a sufficiently general description of the stress–strain behavior of rubber-like networks in different deformation modes was investigated in numerous papers [1,2] and was approached from both the phenomenological and molecular points of view. Our investigation is concerned with the possibility of obtaining an as precise as possible description (with non-systematic deviations less than 10%, preferably less than 5%) of the experimental stress–strain relations in a wide range of biaxial strain (preferably up to break) using constitutive equations based on molecular models. In the present paper, we compare the predictions of the slip-link theory with published biaxial stress–strain data.

The slip-link model was put forward by Ball et al. [3]. It is based on reptation concepts and considers a randomly crosslinked polymer melt where some trapped entanglements between crosslinks are present. At low deformations, the trapped entanglements are able to slide and behave as

slip-links. This leads to a decrease in the reduced tensile stress (strain softening). Making use of the result of Ball et al., Edwards and Vilgis [4] have shown that at high deformations, the trapped entanglements restrict the extensibility and give rise to a strong increase in the elastic stress (strain-hardening). The elastic free energy,  $F(= F_c + F_s)$ , derived from the Edwards–Vilgis (EV) slip-link theory consists of the crosslink part,  $F_c$ , and of the slip-link part,  $F_s$

$$F_c/(N_c kT) = 0.5 \frac{(1 - \alpha^2)I}{Q} + 0.5 \ln Q \quad (1)$$

$$F_s/(N_s kT) = 0.5 \sum_i \left( \frac{P \lambda_i^2}{QR_i} + \ln(R_i) \right) + 0.5 \ln Q \quad (2)$$

where  $I = \sum_i \lambda_i^2$ ,  $Q = 1 - \alpha^2 I$ ,  $R_i = 1 + \eta \lambda_i^2$ ,  $P = (1 - \alpha^2)(1 + \eta)$ .

The summation is performed over the three Cartesian components of the stretch ratio  $\lambda_i$  ( $i = 1, 2, 3$ ).  $N_c$  is the concentration of tetrafunctional network junctions (crosslinks);  $\alpha$ , the inextensibility parameter;  $k$ , the Boltzmann constant;  $T$ , the absolute temperature;  $N_s$ , the concentration of slip-links;  $\eta$ , the slippage parameter, is a relative measure

\* Corresponding author. Tel.: +420-2-2040-3384; fax: +420-2-357-981.  
E-mail address: meissner@imc.cas.cz (B. Meissner).

of the freedom of a link to slide. The inextensibility parameter  $\alpha = b/a$  is predicted to be inversely proportional to the mean distance,  $a$ , between slip-links;  $b$  is the length of the Kuhn segment.

For large extensibilities ( $\alpha = 0$ ),  $F_c$  reduces to the phantom Gaussian result and  $F$  to the result of Ball et al. [3]:

$$F/(kT) = 0.5N_c I + 0.5N_s \sum_i \left( \frac{(1+\eta)\lambda_i^2}{R_i} + \ln R_i \right) \quad (3)$$

A theoretical value of  $\eta = 0.234$  was calculated by Ball et al. with the assumption that each slip-link can on average slide as far as the centers of its topologically neighboring links. Edwards and Vilgis [4] argue that for real situation in a network,  $\eta$  cannot be fixed thus admitting variable values of  $\eta$ . Later on, Vilgis [5] concluded that  $\eta$  should be given by  $(b/a)/N_{pp}$ ;  $N_{pp}$  is the number of slip-links between two crosslinks. With increasing degree of crosslinking,  $N_{pp}$  may be expected to decrease and the slippage parameter to increase.

The principal true stresses,  $t_i$ , can be determined from the elastic free energy to within an arbitrary pressure  $p$

$$t_i = \lambda_i \frac{\partial F}{\partial \lambda_i} + p \quad (4)$$

In order to eliminate the pressure term, the stress–strain relations are frequently written in terms of the difference in the two principal stresses:

$$t_i - t_3 = \lambda_i \frac{\partial F}{\partial \lambda_i} - \lambda_3 \frac{\partial F}{\partial \lambda_3}, \quad i = 1, 2 \quad (5)$$

In a biaxial extension experiment with stresses along the directions 1, 2, the stress  $t_3$  is zero and  $t_i$  follows from Eq. (5). The nominal (engineering) stresses  $\sigma_i$  ( $i = 1, 2$ ) are given by

$$\sigma_i = t_i/\lambda_i \quad (6)$$

Differentiation of  $F_c$ ,  $F_s$  with respect to  $\lambda_i$  yields:

$$\frac{1}{N_c kT} \frac{\partial F_c}{\partial \lambda_i} = \lambda_i \left( \frac{1 - \alpha^2}{Q^2} - \frac{\alpha^2}{Q} \right) \quad (7)$$

$$\frac{1}{N_s kT} \frac{\partial F_s}{\partial \lambda_i} = \lambda_i \left\{ \frac{\alpha^2 P}{Q^2} \left( \sum_i \frac{\lambda_i^2}{R_i} \right) + \frac{P}{QR_i^2} + \frac{\eta}{R_i} - \frac{\alpha^2}{Q} \right\} \quad (8)$$

Using Eqs. (5)–(8), one can calculate the respective homogeneous stresses which are predicted by the EV equation for uniaxial extension (UE), equibiaxial extension (EBE) and pure shear (PS) (for definitions, see Appendix A).

The predictions of Ball et al. for the region of low and medium strains [3] were tested experimentally by Thirion and Weil [6]. They found a good representation of stress–strain data (including the biaxial ones) with  $\eta = 0.4$  and came to the conclusion that a significant fraction of trapped entanglements does not behave as the sliding links of the

model but gives the same contribution to the stress as the chemical crosslinks. The ability of the EV equation to give a satisfactory prediction of both the low-strain softening and the high-strain hardening in UE was shown by Edwards and Vilgis [4] for one natural rubber (NR) network; the authors used the theoretical value of  $\eta = 0.2$  and obtained  $N_s/N_c = 1.75$ ,  $\alpha = 0.133$ . For radiation-crosslinked polyethylene measured in UE above the crystalline melting temperature, Brereton and Klein [7] found a value of the slippage parameter ( $\eta = 1.1$ ) much larger than the theoretical one; it was insensitive to the increase in the radiation dose while parameters  $N_c$ ,  $N_s$ ,  $\alpha$ , showed a tendency to increase. The ratio  $N_s/N_c$  attained high values (30 and more). Bensason et al. [8] studied the tensile stress–strain behavior of elastomeric low-crystallinity ethylene–octene copolymers differing in the degree of crystallinity and molar mass. They conclude that the slip-link theory is able to describe the entire stress–strain curves up to break with a good success and suggest that fringed micellar crystals serve as the multifunctional network junctions, detachment of crystallizable chain segments at the crystal edges provides the sliding mechanism and entanglements of the flexible amorphous chains function as permanent network junctions. Bensason et al. [8] assume that the Brereton and Klein [7] value of  $\eta = 1.1$  is applicable to their polymers and found values of  $N_c kT$  in a relatively narrow range (0.15–0.45 MPa) which were insensitive to the temperature of measurement. Values of  $N_s kT$  ranged from 3 to 20 MPa, showed a tendency to increase with decreasing temperature of measurement and increasing degree of crystallinity; the ratio  $N_s/N_c$  ranged from 10 to 60.

Using tensile measurements on styrene–butadiene networks, Meissner [9] found that the EV equation was able to give a satisfactory fit to some data only, with rather high values of the slippage parameter (1–2) which then necessitated high  $N_s$ . This effect follows from the shape of the EV function: the initial slope of the dependence of the slip-link UE stress on the stretch ratio is given by  $(d\sigma_s/d\lambda)_{\lambda=1} \approx 3N_s kT/(1+\eta)^2$ . Therefore, to satisfy the requirement for a given initial slope, the optimum-fit  $N_s$  must increase with increasing  $\eta$ .

Experimental testing of the slip-link theory carried out so far has been essentially limited to UE data. Comparison with a set of representative biaxial stress–strain data can be expected to lead to a more general and meaningful assessment of the EV model. The parameter estimates obtained will be better substantiated than are those based on tensile data alone and any possible experiment–theory deviations will be revealed more sensitively.

## 2. Comparison of biaxial stress–strain data with the Edwards–Vilgis predictions

Experimental data were taken from several sources (see

Table 1  
Parameter values of the Mooney–Rivlin equation obtained from UE data

Parameter	$2C_{1,MR}$ (MPa)	$2C_{2,MR}$ (MPa)	$C_{2,MR}/C_{1,MR}$
NR-1	0.320	0.190	0.60
NR-2	0.180	0.240	1.33
NR-3	0.145	0.230	1.59
IR	0.220	0.202	0.92
PDMS	0.052	0.057	1.10

Appendix B). Two of them present a full set of biaxial data, one gives UE, EBE, PS measurements up to large strains and two of them comprise UE and EBE data only. The networks used were based on natural rubber, isoprene rubber (IR) and poly(dimethylsiloxane) (PDMS). In the first step, the low- and medium-strain UE data were compared with the Mooney–Rivlin equation [10,11]. Its  $C_{1,MR}$  parameter is often used as a measure of the degree of crosslinking (including both chemical and physical crosslinks). The  $C_{2,MR}$  parameter used to be regarded as a simple measure of the magnitude of deviation from the classical elasticity theory. Values of parameters are given in Table 1. In conformity with previous observations, there is a certain tendency for the ratio  $C_{2,MR}/C_{1,MR}$  to decrease with increasing  $C_{1,MR}$ . It should be recalled that some other networks, e.g. those based on butadiene polymers and copolymers, tend to have higher values of  $C_{2,MR}$  and  $C_{2,MR}/C_{1,MR}$  than isoprene and siloxane networks.

In the second step, the experimental stress–strain data were compared with the predictions of the EV theory using the value of the slippage parameter  $\eta = 0.25$  close to the theoretical one. The remaining three parameters were then adjusted to obtain an as-precise-as-possible description of the data in UE and, simultaneously, minimal data deviations in other deformation modes. In several cases, however, the deviations of data from the fitted curves were systematic and rather large. Therefore, higher values of the slippage parameter were chosen and the procedure repeated in an endeavor to obtain an optimized set of the four parameters. The magnitudes of the relative theory–experiment deviations in different deformation modes and their compromise were taken as a criterion. The values of  $\eta$  were thus estimated with an error of ca.  $\pm 0.1$ . The parameter values

Table 2  
Parameter values of the EV equation obtained from biaxial data

Parameter	$\eta$	$N_c kT$ (MPa)	$N_s kT$ (MPa)	$\alpha$	$N_s/N_c$
NR-1	0.35	0.300	0.310	0.105	1.03
NR-2	0.25	0.210	0.230	0.089	1.1
	1.00	0.205	0.850	0.089	4.15
NR-3	0.50	0.155	0.416	0.104	2.68
IR	0.25	0.249	0.224	0.067	0.90
	0.50	0.265	0.310	0.055	1.17
	0.75	0.268	0.430	0.050	1.60
PDMS	0.25	0.057	0.068	0.053	1.19

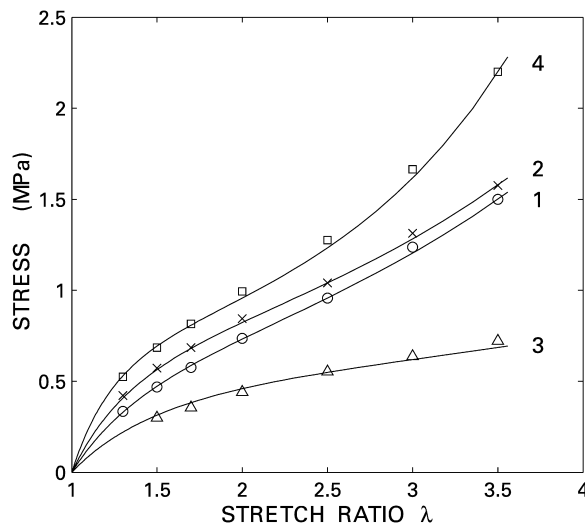


Fig. 1. Comparison of the stress–stretch ratio data with the EV theory. Points: experimental; circles UE, crosses PS1, triangles PS2, squares EBE; NR-1 James et al. [12]. Curves 1 (UE), 2 (PS1), 3 (PS2), 4 (EBE) are drawn according to the EV theory for parameter values given in Table 2.

obtained are summarized in Table 2 and data are compared with the EV predictions in Figs. 1–5.

Fig. 1 shows the data of James et al. [12] on a NR network in the stress–stretch ratio plot. The same data are plotted in Fig. 2 in the form of log (reduced stress) vs. stretch ratio; this type of plot has the advantage of showing the relative

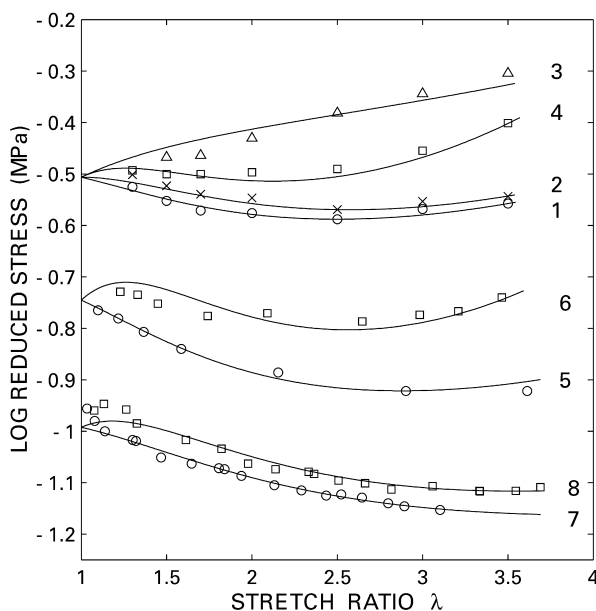


Fig. 2. Comparison of the stress–stretch ratio data (plotted in the coordinates log (reduced stress) vs. stretch ratio) with the predictions of the EV theory. Points: experimental; circles UE, crosses PS1, squares EBE, triangles PS2. Curves 1–4: NR-1 James et al. [12]; curves 5 and 6: NR-3 Rivlin and Saunders [14], UE and EBE data only; curves 7 and 8: PDMS Xu and Mark [16], UE and EBE data only. Curves are drawn according to the EV theory for parameter values given in Table 2. Points and curves 1–4 and 5, 6 are shifted downwards by 0.2 and 0.3, respectively.

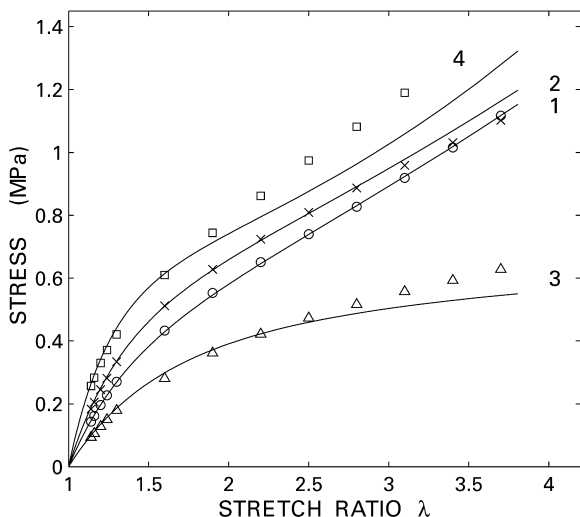


Fig. 3. Comparison of the stress–stretch ratio data with the predictions of the EV theory. Points: experimental; circles UE, crosses PS1, triangles PS2, squares EBE; IR Kawabata et al. [13]. Curves 1 (UE), 2 (PS1), 3 (PS2), 4 (EBE) are drawn according to the EV theory for parameter values given in Table 2,  $\eta = 0.50$ .

experiment–theory deviations with the same sensitivity in the whole range of stretch. Optimum-fit curves are drawn using the appropriate EV equations with  $\eta = 0.35$  (the value is but slightly higher than the theoretical one). The data description can be characterized as good to very good.

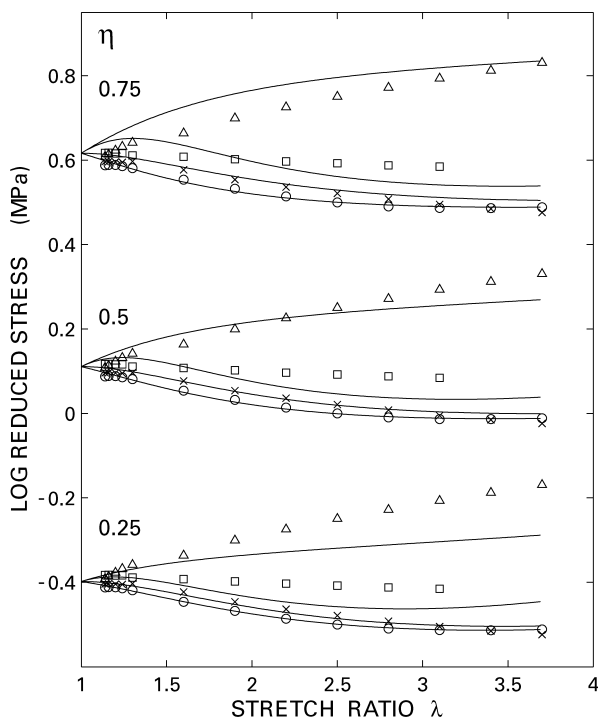


Fig. 4. Data of Fig. 3 plotted in the coordinates of log (reduced stress) vs. stretch ratio. Curves are drawn according to the EV theory for parameter values given in Table 2, values of  $\eta$  are indicated in the graph; points and curves for  $\eta = 0.5$  and  $0.75$  are shifted upwards by  $0.5$  and  $1$ , respectively.

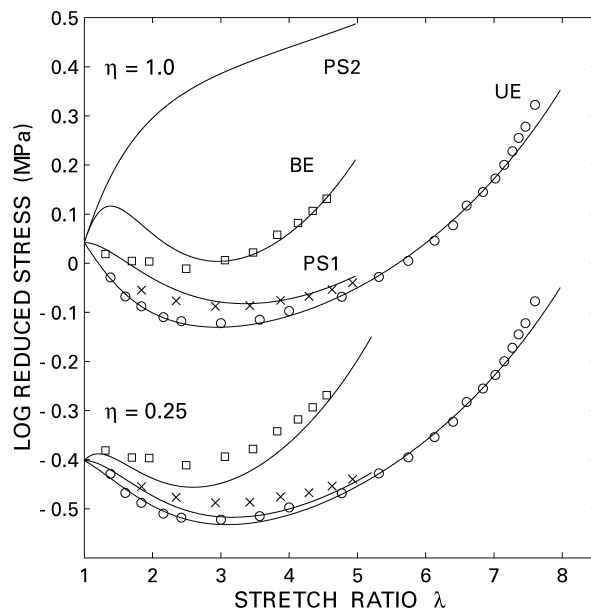


Fig. 5. Comparison of the stress–stretch ratio data (plotted in the coordinates of log (reduced stress) vs. stretch ratio) with the predictions of the EV theory. Points: experimental; circles UE, crosses PS1, squares EBE; NR-2 Treloar [15]. Curves are drawn according to the EV theory for parameter values given in Table 2. Values of  $\eta$  are indicated in the graph. Points and curves for  $\eta = 1$  are shifted upwards by  $0.4$ ; a curve calculated for PS2 is included.

The only deviations larger than 5% (but smaller than 10%) appear in the measurements of  $\sigma_{2,PS}$ .

A similarly successful data description was obtained with lightly crosslinked NR-3 and PDMS networks where, however, only UE and EBE data were available for the test (Fig. 2). On the other hand, systematic and significant deviations ( $\approx 10\%$  or even somewhat higher) from the predictions of the EV theory appear with the data of Kawabata et al. [13] on an isoprene rubber network (Fig. 3). Three values of the slippage parameter were used as starting points for the data–theory comparison (Fig. 4);  $\eta = 0.50$  is clearly better than  $0.25$  and gives a somewhat better compromise than  $\eta = 0.75$ . However, even with  $\eta = 0.50$ , the prediction of the EBE and PS2 data from the UE parameters remains unsatisfactory.

The well-known Treloar data [15] on a NR network with suppressed orientational crystallization are plotted in Fig. 5 in the coordinates of log (reduced stress) vs. stretch ratio. With  $\eta = 0.25$ , the UE curve gives a good fit although the beginning of an increasing deviation appears at the highest stretch ratios. Parameters based on the UE fit, however, give a very poor prediction for the behavior in PS and in EBE. With  $\eta = 1$ , the description of the data in all three deformation modes becomes almost satisfactory and only the low-strain EBE data show a significant deviation (more than 10%). However, the use of a high value for  $\eta$  results in very high values calculated for the PS stress  $\sigma_{2,PS}$ , i.e. for the stress which is required to maintain a unit

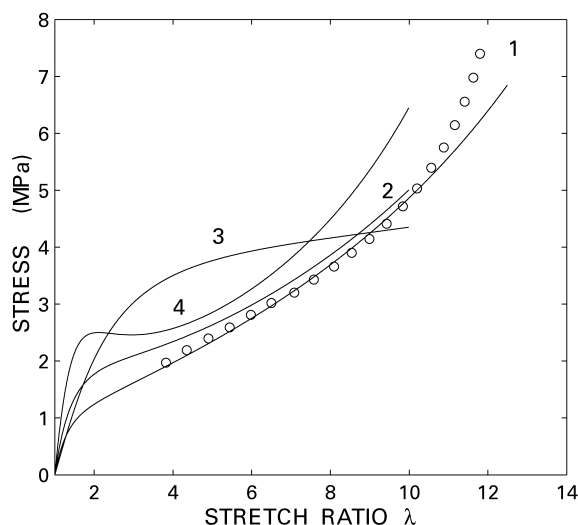


Fig. 6. Comparison of the UE stress–stretch ratio data with the predictions of the EV theory. Points: experimental, ethylene–octene copolymer, Bensason et al. [8]. Curve 1 (UE) is drawn according to the EV theory using the parameter values taken from Ref. [8] and given in the text. Curves 2 (PS1), 3 (PS2), 4 (EBE) were calculated and drawn using the same parameter values.

stretch ratio in the lateral direction while extending the sample in the longitudinal direction to a stretch ratio  $\lambda_1 > 1$  using a stress  $\sigma_{1,PS}$ . For example, for  $\lambda_1 = 2.3$ , the stress  $\sigma_{2,PS} = 0.69$  is *larger* than the stress in UE  $\sigma_{1,UE} = 0.64$  and almost approaches the longitudinal PS stress  $\sigma_{1,PS} = 0.74$ . An even more pronounced effect of this kind follows from the UE data of Bensason et al. [8]; an example of their tensile stress–strain curves is plotted in Fig. 6. It was obtained on an ethylene–octene copolymer with 12.3% of octene,  $M_n = 57$  kg/mol, measured at a strain rate of  $1 \text{ min}^{-1}$  and a temperature of  $40^\circ\text{C}$  where the volume crystallinity was ca. 8%. The EV parameters determined by the authors [8] were  $\eta = 1.1$ ,  $N_c kT = 0.36$  MPa,  $N_s kT = 3.8$  MPa,  $\alpha = 0.033$ . The UE data representation becomes unsatisfactory at high stretch ratios. Using the authors' parameter values and the EV elastic free energy function, we have calculated and plotted the dependencies of the stresses  $\sigma_{1,PS}$ ,  $\sigma_{2,PS}$  and  $\sigma_{1,EBE}$  on the respective stretch ratios  $\lambda_1$  in the same Fig. 6. As it is apparent, the EBE stress shows a maximum. Also, for  $\lambda_1$  values in the 1.6–8.5 range, the  $\sigma_{2,PS}$  stress is predicted to be *higher* than the stress  $\sigma_{1,PS}$ ; e.g. for  $\lambda_1 = 3.5$ ,  $\lambda_2 = 1$ ,  $\sigma_{1,PS} = 7.5$  MPa,  $\sigma_{2,PS} = 17$  MPa (!) is calculated. If now  $\lambda_2$  increases from 1 up to 3.5, while the stretch ratio  $\lambda_1 = 3.5$  is maintained, the stress  $\sigma_{2,PS}$  is predicted to *decrease* from 17 to 10.5 MPa; here, the EBE condition is reached. These predictions do not seem to be realistic and can hardly be expected to be observed experimentally. They follow, however, as a natural consequence from the EV theory which, for the tensile stress supported by slip-links, predicts a dependence with a sharp maximum at low strains. For networks with a low extensibility, the maximum tends to become less

pronounced and may disappear. This explains why the data on the NR-1 network with a high inextensibility parameter can be described fairly well while for a less cross-linked and more extensible IR network a suitable set of parameter values cannot be found.

The comparison of the EV predictions with experimental biaxial data confirms previous conclusions based on uniaxial data [9]. In order to optimize the data description, the slippage parameter must be treated as an adjustable parameter; values in the range between 0.35 and 1 were obtained here. Higher values of the slippage parameter require higher values of  $N_s$ ; e.g. with  $\eta = 1$  for the NR-2 network, the value of  $N_s kT$  becomes more than three times higher than that obtained with  $\eta = 0.25$  and, in addition, it becomes incomparably higher than the  $N_s kT$  values obtained for the other two NR networks. Note also that with optimum  $\eta$ , the ratio  $N_s/N_c$  is practically always higher than  $C_{2,MR}/C_{1,MR}$ , most often much higher. A question arises whether the concentrations of slip-links thus estimated can still be given the physical interpretation suggested by the EV theory. The use of the EV theory for crystalline polymers without taking into account the presence of a non-negligible amount of hard-phase particles is questionable; amplification of strain in the rubbery phase can significantly contribute to the measured stress.

A possible reason for the unsatisfactory ability of the EV equation to give an adequate data description with a satisfactory parameter interpretation in simple one-phase networks can, in principle, be sought in the approximations involved in the mathematical processing of the slip-link model. It should be noted that for the end-to-end distance distribution of a tube-like confined network chain, Edwards and Vilgis intentionally used a simple function; they write [4]: “How can we model the singularity in entropy? There are many possible models (including of course the exact Langevin) but we want a representation which is amenable to calculation and contains the essential features of inextensibility.” Thus, both  $F_c$  given by Eq. (1) and the calculated stresses based on Eq. (1) are to be looked upon as mere approximations of a conceivable rigorous treatment that would model the singularity in chain entropy using Langevin statistics. Such a calculation would probably lead to a function more resembling the result derived by Arruda and Boyce for a network model consisting of eight Langevin chains [17]. The predictions of Edwards and Vilgis for the stress–strain dependencies in UE (for a network without slip-links) and the corresponding predictions of Arruda and Boyce are compared in Fig. 7 under the condition of an equal modulus and equal limiting stretch ratio (locking stretch). The EV stresses (curve 3) are *significantly higher* than the Arruda–Boyce (AB) stresses (curve 2). The finite extensibility contribution to the EV stress seems to be improbably high. For instance, at a stretch ratio of  $\lambda = 5$  and for a locking stretch  $\lambda_{\max} = 8$ , it amounts to 62% of the total stress while the corresponding AB prediction is 28% only. Conversely, if the EV curve is fitted to the AB

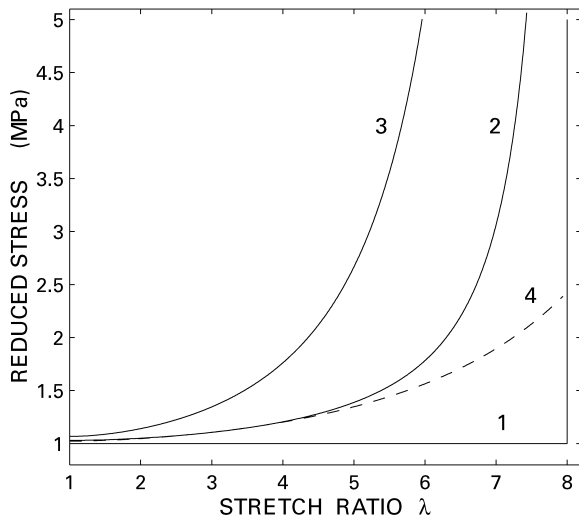


Fig. 7. Comparison of reduced stresses in UE predicted by the Arruda–Boyce and EV theories for a unit modulus and locking stretch  $\eta_{\max} = 8$  (zero concentration of slip-links,  $N_c kT = 1$ ). Curve 1: Gaussian theory, 2: AB theory, 3: EV theory. Curve 4: EV theory, locking stretch  $\eta_{\max} = 13.33$ .

stress up to medium strains (using a lower inextensibility parameter, curve 4), then at high strains the EV stress is lower than the AB stress with the EV locking stretch being higher.

### 3. Conclusion

For networks with low degrees of strain softening and low extensibilities, the EV slip-link theory offers a satisfactory description of published biaxial stress–strain data obtained on simple covalently crosslinked networks, although values obtained for some parameters tend to lie outside the reasonably expected range. For more extensible networks, however, a satisfactory data description was not obtained. The prediction of a pronounced maximum in the strain dependence of stress supported by slip-links seems to be a reason for the discrepancy; it leads to a theoretical expectation that the ratio  $\sigma_{2,PS}/\sigma_{1,PS}$  may assume values higher than unity and this does not seem to be realistic. Also, the modeling of the high-strain singularity in entropy is done in the EV theory using a rather simple approximation and the resulting stress–strain behavior predicted for high strains differs significantly from that following from the rigorously derived Langevin-statistics-based eight-chain-network elasticity theory of Arruda and Boyce.

### Acknowledgements

The authors are greatly indebted to the Grant Agency of the Czech Republic for financial support of this work within the grant project no. 104/00/1311.

Table A1  
Geometry of homogenous deformations

Deformation mode	Stretch ratios	Stresses
UE	$\lambda_2 = \lambda_3; \lambda_3 = 1/\lambda_1^{0.5}$	$\sigma_{1,UE}; \sigma_2 = \sigma_3 = 0$
PS	$\lambda_1 > \lambda_2; \lambda_2 = 1; \lambda_3 = 1/\lambda_1$	$\sigma_{1,PS} > \sigma_{2,PS}; \sigma_3 = 0$
EBE	$\lambda_1 = \lambda_2; \lambda_3 = 1/\lambda_1^2$	$\sigma_{1,EBE} = \sigma_{2,EBE}; \sigma_3 = 0$

Table A2  
Reduced stresses

Mode	Gaussian function	Reduced stress
UE	$\lambda_1 - 1/\lambda_1^2$	$\sigma_{1,UE,red} = \sigma_{1,UE}/(\lambda_1 - 1/\lambda_1^2)$
PS1	$\lambda_1 - 1/\lambda_1^3$	$\sigma_{1,PS,red} = \sigma_{1,PS}/(\lambda_1 - 1/\lambda_1^3)$
PS2	$1 - 1/\lambda_1^2$	$\sigma_{2,PS,red} = \sigma_{2,PS}/(1 - 1/\lambda_1^2)$
EBE	$\lambda_1 - 1/\lambda_1^5$	$\sigma_{1,EBE,red} = \sigma_{1,EBE}/(\lambda_1 - 1/\lambda_1^5)$

## Appendix A

Tables A1 and A2.

### Appendix A.1. Equivalence of EBE and uniaxial compression [1]

In an EBE, the true stress difference  $t_{1,A} - t_{3,A}$  (where equibiaxial true stress  $t_{1,A} = t_{2,A} > 0$ ,  $t_{3,A} = 0$ ) produces stretch ratios  $\lambda_1 = \lambda_2 > 1$ ;  $\lambda_3 = 1/\lambda_1^2 < 1$ . The same set of stretch ratios is produced with the stress difference of the same magnitude ( $t_{1,B} - t_{3,B}$ ) if  $t_{1,B} = t_{2,B} = 0$  and  $t_{3,B} = -t_{1,A} < 0$ , i.e. when using a uniaxial negative (compressive) true stress of the same (absolute) magnitude as was that of the true equibiaxial stress. Moreover, the reduced stress in uniaxial compression,  $\sigma_{UC}/(\lambda_{UC} - 1/\lambda_{UC}^2)$  has the same numerical value as the reduced stress in EBE  $\sigma_{EBE}/(\lambda_{EBE} - 1/\lambda_{EBE}^5)$  if  $\lambda_{EBE} = 1/\lambda_{UC}^{0.5}$ . These relations give an easy way to convert compression data to equibiaxial data and vice versa.

## Appendix B

NR-1 James et al. [12]. Sulfur-accelerator crosslinked natural rubber. The test piece was stress-softened by stretching it 10 times to the maximum deformation. The stretching force was recorded after 5 min relaxation at a given strain.

NR-2 Treloar [15]. Natural rubber crosslinked with a high concentration of sulfur (8 phr) to suppress orientational crystallization. Equilibrium measurements on pre-strained specimens.

NR-3 Rivlin and Saunders [14]. Sulfur-accelerator crosslinked natural rubber.

IR Kawabata et al. [13]. Sulfur-accelerator crosslinked isoprene rubber. Data were taken on pre-strained specimens under equilibrium conditions.

PDMS Xu and Mark [16]. Hydroxy-terminated poly(dimethylsiloxane) (molar mass 21 kg/mol) tetrafunctionally

endlinked with a stoichiometrically equivalent amount of tetraethoxysilane and 0.6 wt% Sn(II) 2-ethylhexanoate as a catalyst. Using increments of load (or inflation pressure), strain was recorded after a sufficiently long time to achieve equilibrium.

## References

- [1] Treloar LRG. The physics of rubber elasticity. 3rd ed. Oxford: Clarendon Press, 1975.
- [2] Erman B, Mark JE. Structure and properties of rubberlike networks. New York: Oxford University Press, 1997.
- [3] Ball RC, Doi M, Edwards SF, Warner M. Polymer 1981;22:1010.
- [4] Edwards SF, Vilgis TA. Polymer 1986;27:483.
- [5] Vilgis TA. Kautsch Gummi Kunstst 1989;42:475.
- [6] Thirion P, Weil T. Polymer 1984;25:609.
- [7] Brereton MG, Klein PG. Polymer 1988;29:970.
- [8] Bensason S, Stepanov EV, Chum S, Hiltner A, Baer E. Macromolecules 1997;30:2436.
- [9] Meissner B. Polymer 2000;41:7827.
- [10] Mooney M. J Appl Phys 1940;11:582.
- [11] Rivlin RS. Phil Trans R Soc Lond, Ser A 1948;241:379.
- [12] James AG, Green A, Simpson GM. J Appl Polym Sci 1975;19:2033.
- [13] Kawabata S, Matsuda M, Kawai H. Macromolecules 1981;14:154.
- [14] Rivlin RS, Saunders DW. Phil Trans R Soc Lond, Ser A 1951;243:251.
- [15] Treloar LRG. Trans Faraday Soc 1944;40:59.
- [16] Xu P, Mark JE. Rubber Chem Technol 1990;63:276.
- [17] Arruda EM, Boyce MC. Mech Phys Solids 1993;41:389.